

## Nonlinear MHD Simulations of ELM Triggering by Pellets in DIII-D and Implications for ITER

S. Futatani<sup>1</sup>, G. Huijsmans<sup>1</sup>, A. Loarte<sup>1</sup>, L.R. Baylor<sup>2</sup>, N. Commaux<sup>2</sup>, T.C. Jernigan<sup>2</sup>, M.E. Fenstermacher<sup>3,4</sup>, C. Lasnier<sup>3,4</sup>, T.H. Osborne<sup>4</sup>, B. Pegourié<sup>5</sup>

<sup>1</sup>*ITER Organization, Route de Vinon sur Verdon, 13115 Saint Paul lez Durance, France*

<sup>2</sup>*Oak Ridge National Laboratory, Oak Ridge, Tennessee 37831, USA*

<sup>3</sup>*Lawrence Livermore National Laboratory, PO Box 808, Livermore, California, 94551 USA*

<sup>4</sup>*General Atomics, P.O. Box 85608, San Diego, California 92186-5608, USA*

<sup>5</sup>*CEA/IRFM, 13108 St Paul lez Durance, France*

### 1. Introduction

ITER operation in the 15 MA  $Q_{DT}=10$  reference scenario is based on the H-mode regime with controlled ELMs (i.e. ELM power losses which do not cause excessive erosion of plasma facing components (PFCs)). Controlled triggering of ELMs by the injection of small pellets has been demonstrated in present experiments as a viable technique to reduce ELM energy fluxes and is one of the ELM control schemes considered for ITER. The application of this technique to ITER requires triggering of ELMs with pellets at frequencies exceeding those of uncontrolled ELMs by a factor of  $\sim 30$ . Uncertainties remain for the practical application of this technique to ITER and, in particular, for the optimization of the pellet characteristics (mass, velocity, injection location) for efficient ELM triggering while minimizing the fuel throughput required by this technique.

In order to provide a firmer physics basis for the triggering of ELMs by pellet injection and to reduce the uncertainties with regards to its application in ITER, non-linear MHD modelling of ELM triggering by pellet injection in DIII-D experiments has been carried out using the non-linear MHD code JOREK [1]. The JOREK code has previously been applied to the simulation of natural ELMs and also to pellet triggered ELMs. In previous studies, the pellet was modelled as a strongly localized instantaneous density source with a constant amplitude and position [1]. For the work presented here, a pellet ablation model (the neutral gas shielding (NGS) model [2]) has been implemented in JOREK as a moving and time-varying, toroidally and poloidally localised, adiabatic density source.

### 2. Simulation Setup

As an initial condition, the DIII-D ITER-like equilibrium (shot no. 131498,  $q_{95}=3.5$ ,  $\beta_N=1.8$ ,  $H_{98}=1.1$ ) is used. The pedestal plasma is reproduced with JOREK by a suitable choice of the radial dependence of the diffusion coefficients. Modelling of natural (or uncontrolled) ELMs has been carried out for DIII-D to verify that the edge plasma in these discharges becomes MHD unstable leading to the occurrence of an ELM, once the pedestal plasma parameters reach the measured pre-ELM conditions [3]. Figure 1 shows results of the JOREK simulation of the density perturbation and flow contours due to unstable ballooning modes in the DIII-D ITER-like plasma [3]. Modelling of pellet triggered ELMs in DIII-D has been carried out by simulating the injection of pellets at an earlier time in the natural ELM cycle, when the plasma pedestal pressure is 70% of its maximum value so that, in the absence of the pellet perturbation, the plasma is MHD stable. Pellet injection has been simulated for velocities in the range of  $25-100 \text{ ms}^{-1}$  and for cylindrical sizes from 1.0 to 2.7 mm. Figure 2(a) shows typical profiles of the ablation rate, which is based on the NGS model, for a pellet injected from the midplane with a velocity of  $100 \text{ ms}^{-1}$ . The ablation rate is strongly dependent on the plasma temperature.

### 3. ELM triggering, dependence on the pellet size

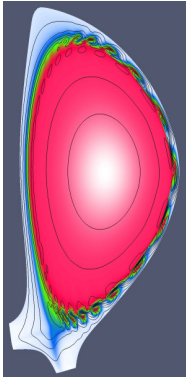


Figure 1. Modelled plasma density (in colour) and flow contours (lines) during an uncontrolled ELM in ITER-like DIII-D plasma.

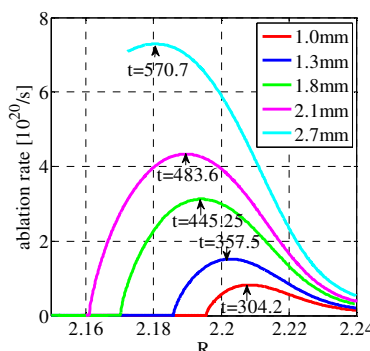
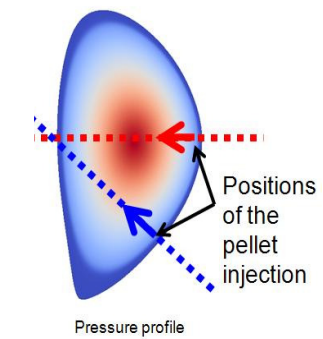


Figure 2. (left) Pellet ablation rate [ $10^{20}/s$ ] for four different pellet sizes (1.0mm, 1.3mm, 1.8mm and 2.1mm) as a function of the plasma radius; (right). Illustration of the two pellet injection geometries considered, from midplane and from X-point region.



To determine the requirements of the pellet parameters for the triggering of ELMs in DIII-D, cylindrical pellet sizes with diameters of 1.0, 1.3, 1.8, 2.1 and 2.7 mm, are simulated with an injection velocity of  $100 \text{ ms}^{-1}$  at the outboard midplane. In order to ease the numerical modelling, only the plasma inside of the separatrix has been studied. The ablating pellet source leads to a large density perturbation expanding in the parallel direction close to the local sound speed. Due to the large parallel heat conductivity in the confined plasma, even though the density rises to much higher values as the pellet ablates, the temperature decrease is limited, resulting in a large local pressure increase near the pellet injection location. The ELM is triggered when the toroidally localized pressure (gradient) exceeds a critical value during the ablation process. Figure 3(a) shows the time evolution of the magnetic energy (toroidal modes  $n=6-10$ ) for several pellet sizes. The strong growth of the energy is the signature of ELM triggering which can only be observed for larger pellets ( $\geq 1.8\text{mm}$ ). Smaller pellets ( $\leq 1.3\text{mm}$ ) induce a magnetic perturbation, but strong energy growth does not occur and, after the pellet is fully ablated, the MHD activity relaxes. In order to quantitatively determine in the simulation when an ELM has been triggered by a pellet, the total magnetic energy of the most unstable modes ( $n=6-10$ ) is plotted against the pellet particle source, see Fig. 3(b). For small pellet sizes ( $< 1.3 \text{ mm}$  in this case) the total magnetic energy increases quadratically in time with the particle source deposited in the plasma until the pellet is fully ablated, which is in agreement

with previous results with a simple pellet model [1]. However, for larger pellets ( $\geq 1.8 \text{ mm}$  in this case), the total magnetic energy grows initially quadratically with the pellet ablated source until a point in time where its growth becomes much larger. This is interpreted as the beginning of the ELM triggered by the pellet. JOREK modelling shows that the key-parameter for ELM triggering is the local plasma pressure perturbation caused by the pellet. As shown in Fig. 4(a), for the larger pellet sizes ( $\geq 1.8\text{mm}$ ), the plasma pressure profiles

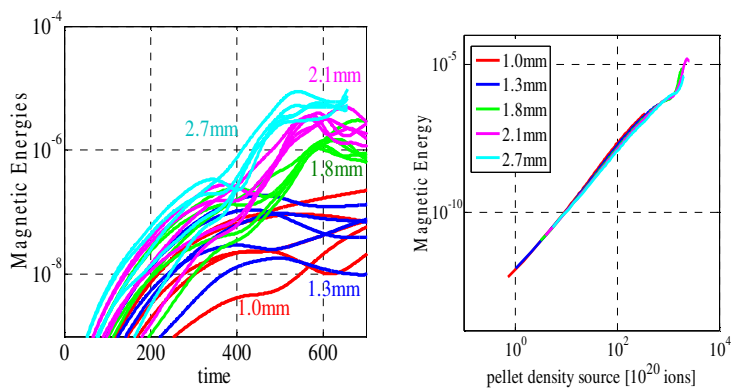


Figure 3. (left) The time evolution of the magnetic energies for toroidal harmonics of  $n=6-10$ ; (right) Total magnetic (addition of  $n=6-10$  harmonics) energy versus pellet density source.

at the time of the ELM onset are very similar. In these simulations, the ELM is triggered when the pellet is near/beyond the top of the pedestal and the pressure gradient in the pedestal region adds to the pellet induced pressure gradient. Smaller pellets ( $\leq 1.3\text{mm}$ ) show the typical linear MHD response of the plasma to the pellet but no MHD instability and thus no ELM occurs. This comparison shows that ELM triggering by pellets in DIII-D for ITER-like plasma discharges requires the local plasma pressure in the pedestal region to exceed a given threshold value (40 kPa in these simulations); otherwise the initial MHD perturbation caused by the pellet relaxes without triggering ELMs. This pressure threshold criterion for ELM triggering leads to a minimum pellet size being required for triggering of ELMs for a given set of pedestal parameters, pellet velocity and injection geometry.

#### 4. ELM triggering, dependence on pellet injection geometry

The effect of the location of pellet injection has been studied for injection near the mid-plane and near the X-point with the same plasma shape as [3], as shown in Fig. 2(b). The simulations reveal some commonalities and three important differences regarding ELM triggering. In the first place, it is found that for both geometries a minimum local pressure (or gradient) must be reached after the pellet is injected for the ELM to be triggered. However, the size and position of the pressure perturbation and the minimum pellet size required for pellet triggering are different for the two injection geometries, as shown in Fig. 4. X-point injection leads to ELMs being triggered when the pressure perturbation is localised further out in the pedestal region than for mid-plane injection and the magnitude of the pressure perturbation required is about 20% lower for the X-point injection. In addition, the X-point geometry allows ELMs to be triggered with a smaller pellet size (1.3 mm) than that required for midplane injection (1.8 mm). This may result from a combination of various effects which are under investigation : a) the larger flux expansion of the plasma along the pellet trajectory leading to a larger ablation rate and pellet pressure perturbation in the edge gradient region, so that the local pressure gradient caused by the pellet and the background plasma pressure gradient add more effectively, b) due to the long connection length and flux expansion near the X-point, the high density cloud created by the pellet remains for a longer time in this region than when injected at the midplane giving a longer-lived trigger for the MHD instability for X-point injection and c) the MHD response of the plasma to a perturbation in the X-point region maybe different than that near the midplane. Whatever is the key driving physics mechanism for this behaviour, JOREK modelling indicates that pellet injection near the X-point (as adopted for ITER and demonstrated in DIII-D) should ease the pellet size requirements for ELM triggering in ITER.

#### 5. ELM triggering dependence on pellet speed

The dependence of ELM triggering on pellet speed (in the range of  $25\text{-}100\text{ ms}^{-1}$ ) has been simulated for a pellet size of 1.8 mm injected at the midplane. At low velocity ( $25\text{ ms}^{-1}$ ), the pellet is fully ablated in the pedestal region and leads to the maximum pressure perturbation to occur in the pedestal region, thus triggering the ELM at a slightly lower peak pressure (similar to the effect seen for the X-point injection).

#### 6. Modelling of ELM triggering by pellet pacing with divertor geometry

In order to evaluate the heat and particles fluxes associated with pellet pacing on the divertor targets, the simulation region has been extended to the include the full plasma and SOL geometry. So far, the studies have been carried out for pellets injected from the midplane with a velocity of  $100\text{ ms}^{-1}$  and the pellet size has been scanned. The dependence of ELM triggering on pellet size is virtually identical to those described in section 3. Figure 5 shows snapshots of plasma density (in colour) and flow contours (in lines) for (a) 1.0mm and (b) 2.1mm pellet injected in DIII-D. The smaller pellet (Fig. 5.a) does not produce the growth of a peeling-balloonning mode structure and triggering of an ELM while the larger pellet destabilizes peeling-balloonning modes and causes the expulsion of plasma density in the form

of filaments (see Fig. 5.b). Following the growth of the MHD instability, the heat flux to the divertor increases as shown in Fig. 6. JOREK simulations of natural ELMs and pellet triggered ELMs reproduce some of the features (but not all) seen in the experiment. Pellet triggered ELMs lead to a lower peak heat flux and a longer ELM power deposition timescale at the inner and outer divertor than natural ELMs. In addition, the divertor power flux for pellet-triggered ELMs shows a doubly-peaked structure with  $n=1$  toroidal symmetry, unlike the multiply-peaked structure observed during the modelled natural ELMs, in agreement with measurements at JET [4]. For pellet triggered ELMs, the widest radial separation between the peaks occurring at the toroidal angle opposite to that of the injected pellet, as shown in Fig. 7. This is in agreement with measurements at JET [4]. On the other hand, as shown in Fig. 6, JOREK simulations for natural and pellet-triggered ELMs show a predominant power flow towards the outer divertor, which is not found in the experiment [3].

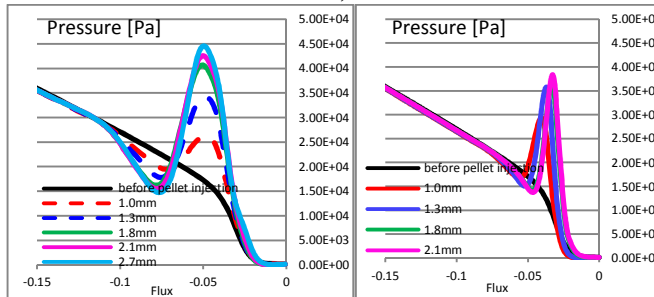


Figure 4. Pressure perturbations when the ELM is triggered for two cases of the pellet injection geometry; midplane (left) and X-point region (right). Dashed lines correspond to the maximum pressure for pellet sizes for which no ELM is triggered.

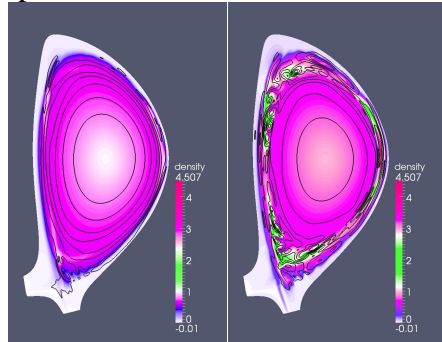


Figure 5. Modelled plasma density (in colour) and flow contours (lines) after the pellet injection (left: 1.0mm, right: 2.1mm)

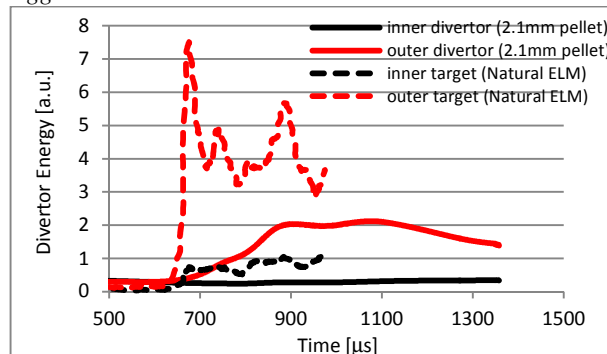


Figure 6. Heat flux to the inner and out divertor versus time. Black lines correspond to the inner divertor while red lines are outer divertor. Dashed lines correspond to a natural ELM while solid lines correspond to a pellet (2.1 mm) triggered ELM.

**Acknowledgment:** This work was supported in part by the US DOE under DE-AC05-00OR22725, DE- AC52-07NA27344, and DE-FC02-04ER54698.

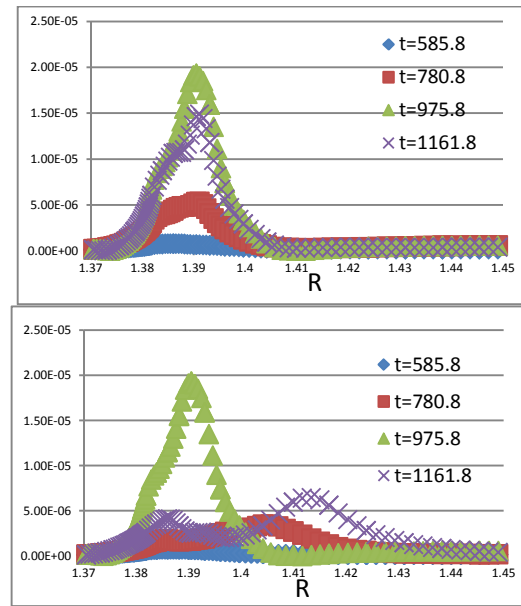


Figure 7. Profiles of the divertor heat flux on the target for (top) the toroidal location of pellet injection and (bottom) the toroidally opposite location of pellet injection.

**Disclaimer:** The views and opinions expressed herein do not necessarily reflect those of the ITER Organization.

## References

- [1] Huysmans, G.T.A., et al., *Plasma Phys. Control. Fusion* **51** (2009) 124012.
- [2] Gal, K., et al. *Nucl. Fusion* **48** (2008) 085005.
- [3] Baylor, L.R., et al., *Proc. 2012 EPS Conference*, Stockholm, Sweden, 2012.
- [4] Wenninger, R.P., et al., *Plasma Phys. Control. Fusion* **53** (2011) 105002.